Proceedings of Computational Engineering Conference JSCES
Vol. 28, 2023 May

Fluid-Structure Interaction of a Cropped Delta Wing in Transonic Regime

Sheila C.F. Langa[1)] and Yusuke Takahashi[2)]

1) Graduate Student, Graduate School of Engineering (Hokkaido University, E-mail: sheilachicafrancisco.langa.b0@elms.ac.jp)
2) Associate Professor, Faculty of Engineering (Hokkaido University, E-mail: ytakahashi@eng.hokudai.ac.jp)

In the present study, the aeroelastic flutter and limit-cycle oscillation (LCO) of a cropped delta wing were analyzed using a Fluid-Structure Interaction (FSI) model. The FSI model consisted of open-source software (OSS) namely SU2 as a fluid solver, CalculiX as a structural solver, and preCICE as the coupling library. The FSI analysis was conducted over a range of different dynamic pressures. It was found that the nonlinearities in the fluid model had more impact on the LCO phenomena and that the leading motion of the wing was governed by the first bending mode. When compared to the experimental and other numerical results, the current model was found to be in better agreement with previous numerical computations than with experimental measurements.

Key Words : *Fluid-structure interaction, Limit-cycle oscillation, Cropped delta wing, Transonic flow*

1. INTRODUCTION

High maneuverability and increased flexibility in aircraft wings have been some of the main criteria in recent wing design applications. Wings that account for such configurations are prone to aeroelastic behavior. Aeroelasticity is a subsection of Fluid-Structure Interaction (FSI), and is caused by the interaction between the inertial, aerodynamics and elastic forces [1]. Aeroelastic analyses in high-speed flow, such as in the transonic region, are very complex due to the inherent nonlinearities [2] of the flow. One of the most challenging transonic aeroelastic phenomena is called flutter. Flutter is a self-excited oscillation that results from the nonlinear interaction of the unsteady aerodynamics and structural vibrations in the system. When this oscillation has a limiting amplitude, it is regarded as Limit-Cycle Oscillation (LCO). LCO is mainly caused by the nonlinearities present in the aeroelastic system which could be due to the flow aerodynamics, the structural response, or both [1,3]. Approaching to capture wing LCO using classical linear flutter techniques has proved to be inadequate [2]. Additionally, performing wind-tunnel FSI tests is highly difficult since it is challenging to reproduce the accurate flow and structure conditions with respect to the scaling law. Thus, to accurately capture the physics of the flow [4], numerical nonlinear aeroelastic analyses should be performed taking into consideration the nonlinearities of the fluid and the structural counterparts in a coupled manner.

The current study presents an FSI analysis of a non-slender cropped delta wing model with geometric plate nonlinearities [1] which is prone to transonic flutter and LCO occurrence. This wing model was experimented by Schairer and Hand [5]. It has also been numerically examined by Gordnier et al. [6], in which the LCO behavior was found to be caused by the leading-edge vortex which behaved as an aerodynamic spring, and again in [7] where it was concluded that geometrical nonlinearities played a major role in the LCO mechanism. Attar et al. [3] determined the importance of properly and accurately modeling the fluid and structural problems. Cui et al. [8] concluded that alongside geometric nonlinearities, material nonlinearities should also be considered when analyzing the model for better accuracy in terms of LCO amplitude. While the mentioned studies [3,6-8] apply structured grids for the FSI analysis, this research aims to use fully unstructured grid models to analyze the impact of grid refinement techniques on the flow behavior as well as on the LCO mechanism.

Although numerical analyses of FSI require high computational resources, recent advances in computational methods have enabled the convenient modeling of FSI simulation. One of the advances being the development of a multi-physics coupling library called preCICE [9]. preCICE is an open-source software (OSS) which is able to couple sophisticated single-physics software by means of adapters [9,10]. Various adapters have already been implemented for preCICE such as the fluid solver SU2 [11], and the nonlinear structural solver Calculix [12] which comprise the proposed FSI model of this analysis. This fully OSS-based model consisting of SU2, CalculiX and preCICE has been chosen due to its high degree of freedom [10].

The focus of the present study is to analyze the LCO behavior of the delta wing configuration in transonic regime using partitioned-coupling OSS-based FSI with fully unstructured grid models. The results aim to establish a validation between the experimental data [5] and comparison with the numerical studies [3,8] to ensure FSI coupling validity.

2. FSI MODEL

The current FSI analysis model consists of SU2 as the aerodynamics solver based on a finite volume method, CalculiX as the nonlinear structural mechanics solver based on the finite element method, and preCICE as the coupling library.

(1) Cropped Delta Wing

The target analysis object of this study is a cropped delta wing model with zero angle of attack placed in freestream transonic flow. The wing model geometry is displayed in Fig.1. The wing has a root length, semi-span length and thickness of 0.29845 m, 0.2032 m, and 0.000889 m respectively. Additionally, it has a leading-edge sweep of 47.8° and a trailing edge sweep of -8.7°.

(2) Aerodynamic Solver

The unstructured-mesh fluid flow solver, SU2, is used in this

numerical investigation. The governing equations are the compressible Navier-Stokes equations consisting of momentum, total density, and total energy conservation laws. The Navier-Stokes equations were discretized using the finite volume approach. Additionally, the ideal gas equation of state is also included in the governing equations. The ideal gas thermodynamic properties of the airflow are considered to be the same as those of standard air.

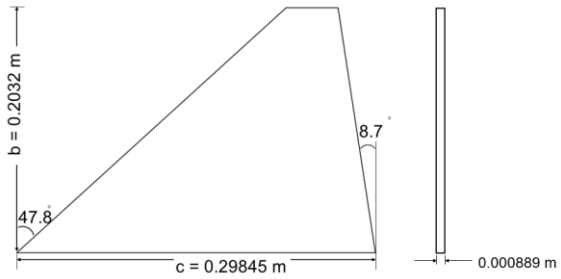

Fig.1 Wing Geometry

The viscosity coefficients are evaluated by the Sutherland's viscosity model as well as the Constant viscosity model, and a Prandtl number of 0.72 is used. Turbulence models are not assumed in the present analysis. The Jameson Schmidt Turkel (JST) scheme [13] is used for the evaluation of the advection term, and the Green-Gauss method is used to calculate the spatial gradients. The computations for unsteady states were performed by using an implicit dual-time stepping time integration based on the 2nd order backward difference. For the inner iterations, local time stepping is used, and for the outer iterations, global time stepping is used. The coefficient matrix solution method is performed by the FGMRES method with the incorporation of the lower-upper symmetric Gauss-Seidel (LU-SGS) method for preprocessing.

(3) Structural Mechanics Solver

The open-source structural solver based on finite-element method, CalculiX, is used in this study. The cropped delta wing was modeled as a three-dimensional object with linear material properties. The structural dynamics are solved based on the principle of virtual work. The momentum equilibrium of the displacement field was obtained under the assumption that there is no temperature change inside the model. The governing equation is discretized by small elements and consists of the element mass matrix, the element stiffness matrix, the element load vector, and the element displacement. By using the shape function incorporated in the formulation of the element stiffness matrix, the element mass matrix was calculated. The load vector, the mass matrix, and stiffness equation were obtained by defining a displacement load vector. The stiffness equation is solved by using the Gauss-Legendre quadrature with the α −method [14].

(4) Coupling Method

The current numerical model uses a partitioned coupling approach through the preCICE library. The fluid and structural analyses are independently solved and then coupled at the interface. From the fluid solver, the aerodynamic forces on a coupling boundary are transmitted. On the other hand, the structural solver transmits the displacements. This coupling mechanism does not require the computational grids to be the same at the interface. Even so, the data mapping is interpolated appropriately using the nearest-neighbor mapping technique. Finally, the equilibrium and continuity constraints on the coupling boundary are satisfied through the implementation of a parallel-implicit scheme.

(5) Computational Conditions

Previous computations [3,8] use structured grids for both the fluid and structural grids. Given that both SU2 and CalculiX use unstructured grids, two refinement mechanisms are presented for each of the solvers to properly understand the impact of meshing strategies in the flow solution. They are paired in sets based on the refinement level. Fig.2 shows one coarse structural grid with122,626 nodes, and a coarse fluid grid with 682,546 cells. On the other hand, Fig.3 presents a refined structured grid with 270,762 nodes, and a refined fluid grid with 5,217,900 cells.

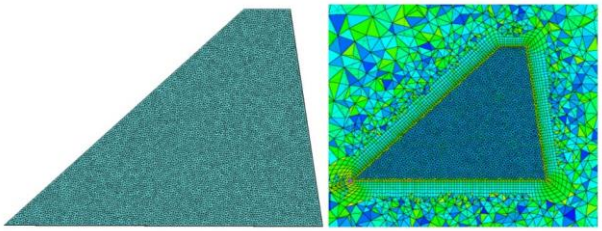

Fig. 2 Coarse grids

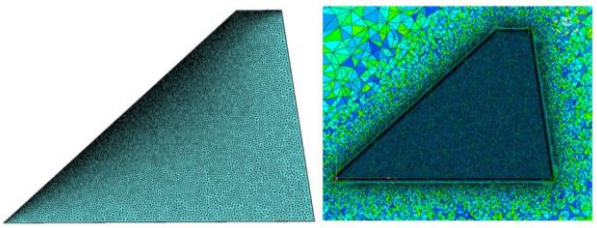

Fig. 3 Refined grids

For both cases, the angle of attack is set to zero and the freestream conditions are considered. The freestream conditions are evaluated from the isentropic process. No-slip conditions and no pressure gradient to the normal direction at the wing surface are assumed.

All the surfaces of the wing are set to be coupled interfaces. The analysis is performed by changing the freestream dynamic pressures from 20.54 to 26.75 kPa and the Reynolds length is fixed at 0.298 m.

The structural meshes are fixed at the bottom while all the other surfaces are allowed to move freely. The delta wing is considered to be of a single material with material properties close to cold-rolled steel which was used in the experiment [5] with Young's modulus of 206GPa, Poisson's ratio of 0.25 and density of 7,833 kg/m^3.

The coarse grid pair uses the viscosity term by Sutherland's law. For the implementation of the adequate transonic flow, a constant freestream Mach number of 0.9, velocity of 290.028 m/s, and temperature of 257.996 K. Here, the freestream Reynold's number differs slightly in comparison to those of the experiment [5]. As for the refined grid set, a constant viscosity model is used with 1.4 x 10^5 kg/ms and the experimental Mach number and Reynold's number are ensured. Table 1 shows a brief outline of the difference in Reynolds number based on the viscosity model applied in SU2 with comparison to the experiment [5]. For both cases, no turbulence modeling is used.

Table 1 Freestream condition for flow field

q kPa (Exp.)	Mach (Exp.)	Re x 10^6 (Exp.)	Re x 10^6 (Sutherland)	Re x 10^6 (Constant)
20.54	0.874	3.15	2.57	3.15
21.72	0.872	3.36	2.72	3.36
22.96	0.869	3.56	2.88	3.56
23.79	0.860	3.56	2.98	3.56
26.75	0.860	3.72	3.35	3.72

3. RESULTS AND DISCUSSION

In this section, the results of the eigenfrequency study are outlined, followed by a discussion on the FSI behavior of the wing in the transonic flow. Additionally, the impact of the meshing strategies and flow properties will be discussed.

(1) Eigenfrequency Analysis

An eigenfrequency study based on the finite element method was performed by solving the equation below.

$$Kx = \lambda Mx \tag{1}$$

Where K is the overall stiffness matrix, M is the overall mass matrix, x is the eigenvector, and λ is the eigenvalue. This vibration analysis was performed using CalculiX. Table 2 includes the results for modes 1 to 3 in comparison to the experiment.

Table 2 Eigenfrequency comparison

Modes	Experiment [5] (Hz)	Coarse (Hz)	Refined (Hz)
1	26.7	26.70	26.70
2	88.2	89.25	89.27
3	131.8	133.44	133.47

Regardless of the refinement mechanism, the frequencies for the first mode were the same as that of the experiment which is 26.7 Hz. For modes 2 and 3, both meshes show slightly larger frequencies, around 89 Hz and 133 Hz in contrast with 88.2 and 131.8 Hz from the experiment [5]. Nevertheless, the main motions of the wing were consistent with the experiment and numerical computations with mode 1 set to first bending, mode 2 set to first torsion and mode 3 set to second bending, thus ensuring the validity of the structural models. Fig.4 shows a side-by-side visual comparison of eigenfrequency modes of the coarse grid and the experiment [5].

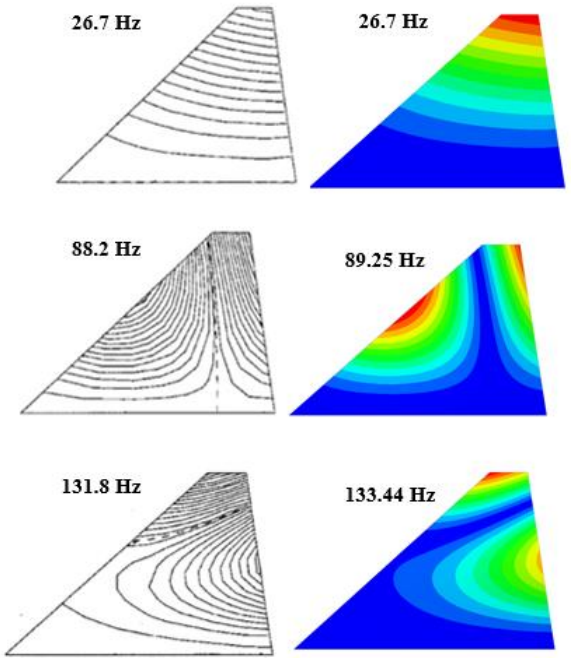

Fig. 4 Mode shapes

(2) LCO Analysis

The time and history of displacement were examined by inserting probes at the trailing edge of the cropped delta wing at (0.26735, 0.2032, 0). The displacement history for 5 different dynamic pressures which are 20.54, 21.72, 22.96, 23.79, and 26.75 kPa were analyzed.

The self-excited limit-cycle oscillation occurs when the airflow is generated at the stationary wing. For all the cases, a constant growth in LCO displacement is observed as the dynamic pressure is increased. Similarly to the experiment and computations [3,5,8], the leading motion of the wing was observed to be the first bending mode.

The coarse mesh model showed stable oscillations. For the case of 21.72 kPa, the displacement gradually expands until it reaches the LCO, thus resembling a Van der Pol oscillation phenomenon. For the cases of 22.92 to 26.75 kPa there is a rapid increase in amplitude followed by strong damping until LCO is reached. However, the LCO frequencies were extremely small when compared to the experimental ones.

The refined mesh model showed rather large LCO displacement in comparison to the coarse mesh model, however the LCO phenomena seemed rather unstable in comparison. Brief comparisons on 20.54, 21.72, and 22.96 kPa are shown in Fig. 5.

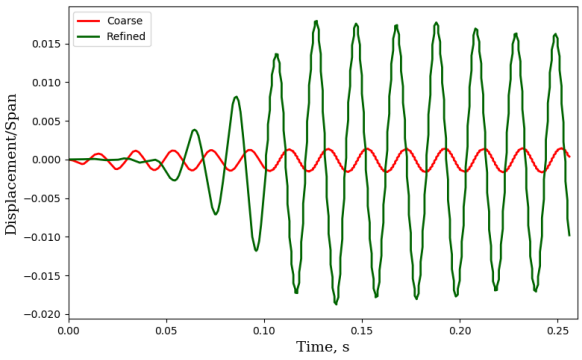

(a) Displacement at 20.54 kPa

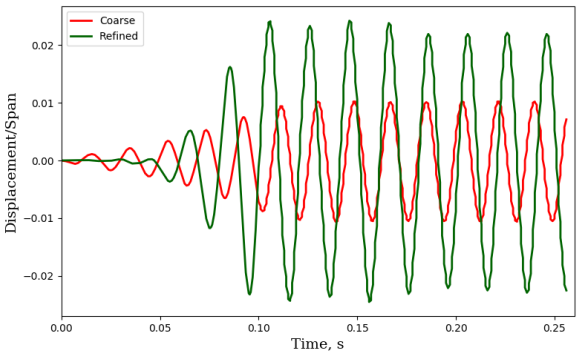

(b) Displacement at 21.72 kPa

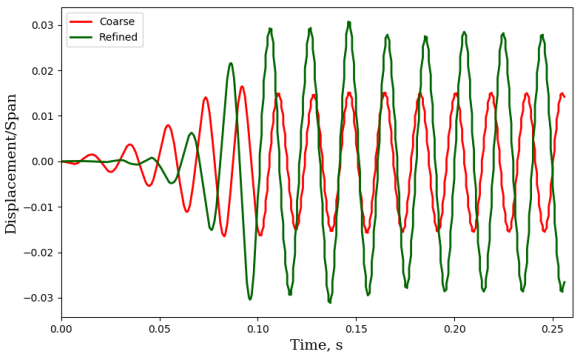

(c) Displacement at 22.96 kPa

Fig. 5 Wing tip displacement comparison

To obtain the LCO frequencies, a Fast Fourier Transform (FFT) analysis was performed on displacement data. The peak

frequencies for the coarse mesh were 50.8, 54.7, and 58.6 Hz. On the other hand, the peak frequencies for the refined mesh were 46.9 and 50.8 Hz. Although the refined mesh frequencies do not strictly match the experimental results [5], they were found to be in better agreement with Attar et al.'s [3] research. This result is consistent with the expectations, given that similarly to Attar, no material nonlinearities were included in the model. The fact that the LCO frequencies are not the same with the eigenfrequency results suggest that the main reason behind the LCO mechanism in the current model is caused by an external aerodynamic force. Frequency results are shown for the coarse and refined mesh at 21.72 kPa in Fig.6 (a) and (b) respectively.

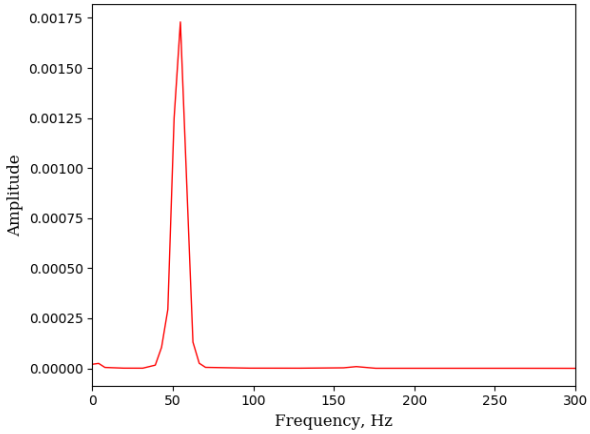

(a) LCO frequency for coarse mesh at 21.72 kPa

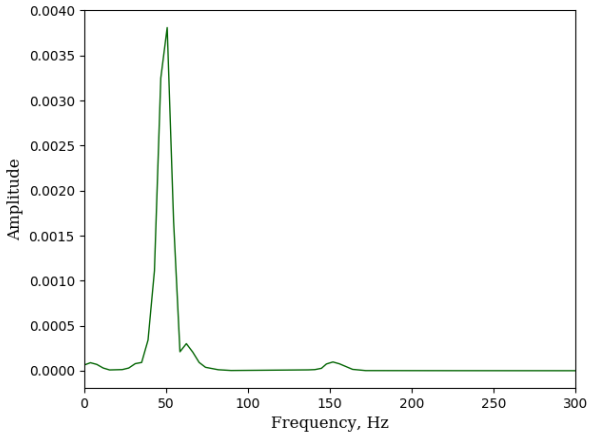

(b) LCO frequency for refined mesh at 21.72 kPa

Fig 6. LCO frequency at 21.72 kPa

Additionally, a general comparison of the LCO frequency and wingtip displacement with the experiment and numerical computations are shown on Fig. 7 and Fig.8 respectively.

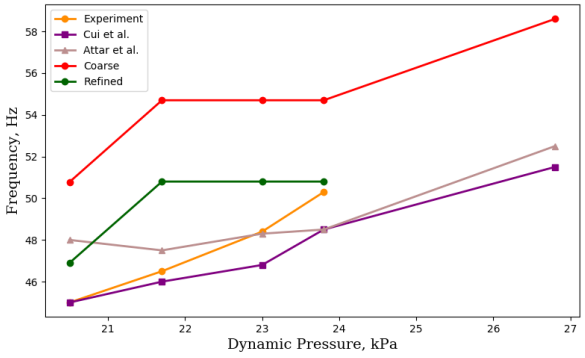

Fig 7. LCO frequency comparison

In the comparison shown on Fig.7, an odd behavior is seen. Rather than a constant increase in frequency, a constant frequency is seen between 21.72 to 26.75 kPa. The reason behind this behavior does not have to do with neither the viscosity models nor the refinement techniques, given that both mesh models showed the same trend. Additionally, it could be argued that the difference in meshing strategy, unstructured in this case, could have played a role on this constant frequency range. The investigation of such a behavior is the scope of future work.

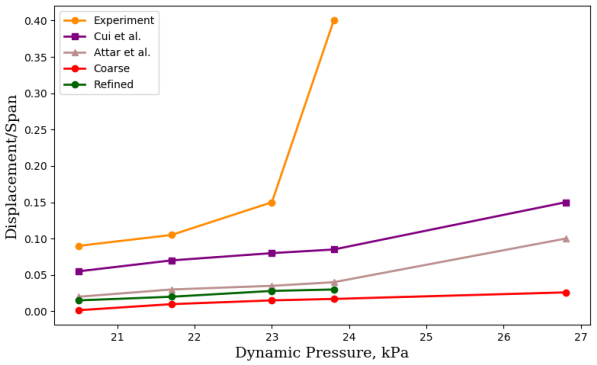

Fig 8. LCO displacement comparison

(3) Aerodynamic Analysis

The difference in refinement mesh techniques gave an insight on the importance of the mesh in order to capture important physical behavior in the wing surface. Fig.9 (a) and (b) show the pressure coefficient distribution on the wing surface for 22.96 kPa. It is clearly visible that for the same dynamic pressure, the refined mesh, in Fig. 9 (b) shows a vortex breakdown around the leading edge of the wing. Additionally, a slight shock wave motion moving from the trailing edge to the leading edge is observed.

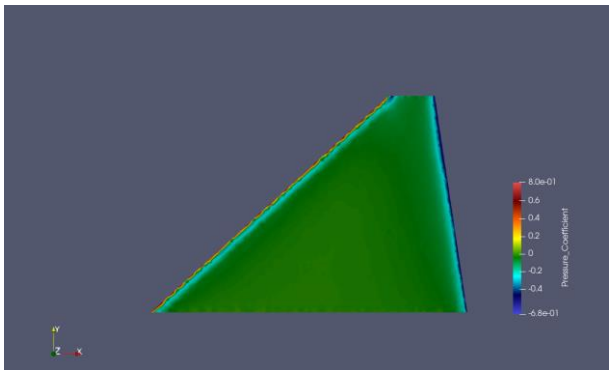

(a) Coarse mesh pressure coefficient distribution

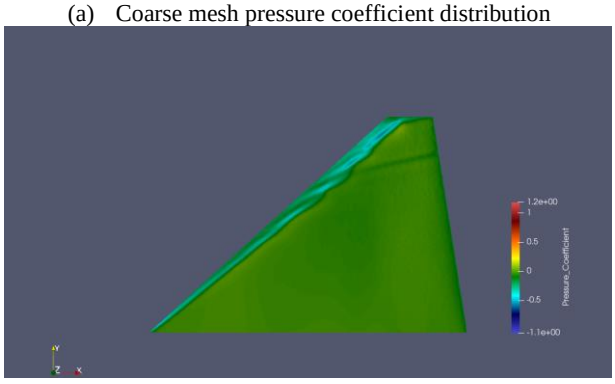

(b) Refined mesh pressure coefficient distribution

Fig. 9 Pressure Coefficient distribution at 22.96 kPa

This vortex breakdown and shock wave motion could play a considerable role in the unstable nature of the LCO amplitude for the refined mesh case and is in closer proximity with previous computational studies [3,8].

The implementation of better refinement meshing techniques around the wing tip should be considered in future research.

4. CONCLUSIONS

In the present work, an open-source software-based fluid-structure interaction (FSI) model was constructed. The FSI analysis was performed in a partitioned-coupled manner on a LCO-prone cropped delta wing model in the transonic speed region. The FSI analysis consisted of a finite volume approach for the fluid solver and a finite element approach for the structural solver which were coupled at a coupling library.

Two meshing strategies and viscosity models were presented in order to clarify the difference in results between the current model with the experiment and previous computational studies. It was found that the LCO displacement increased as the dynamic pressure was increased and that the leading motion was the first bending mode, thus agreeing with the experimental and numerical data. The discrepancy in the frequencies found by the modal analysis in contrast to those of the FSI analysis suggest that an external aerodynamic force is behind the LCO mechanism of the wing. The refined mesh model displayed some vortex breakdown accompanied with some shock wave motion whereas such flow behavior was not seen for the coarse mesh model. This validated that meshing techniques also affect the physical flow properties. Additionally, the LCO frequency was observed to have constant values over a certain range of dynamic frequencies. This unusual behavior of the frequency needs further investigation and is the scope of future work.

REFERENCES

[1] Dowell, E. H.: A Modern Course in Aeroelasticity, 6th edition, 2022.

[2] Bendiksen, O.O.: Review of unsteady transonic aerodynamics: Theory and applications, *Progress in Aerospace Sciences*, 47(2), 135-167, 2011.

[3] Attar, P.J. and Gordnier R.E.: Aeroelastic prediction of the limit cycle oscillations of a cropped delta wing, *Journal of Fluids and Structures*, 22(1), pp.45-58, 2006.

[4] Gursul, I., Gordnier, R.E. and Visbal, M.: Unsteady aerodynamics of nonslender delta wings, *Progress in Aerospace Series*, 41(7), pp.515-557, 2005.

[5] Schairer, E.T. and Hand, L.A.: Measurements of unsteady aeroelastic model deformation by stereo photogrammetry, *Journal of Aircraft*, 36 (6), pp.1033-1040, 1999.

[6] Gordnier, R.E. and Melville, R.B.: Physical mechanisms for limit-cycle oscillations of a cropped delta wing, *30th AIAA Fluid Dynamics Conference*, p. 3796, 1999.

[7] Gordnier, R.E., Computation of limit cycle oscillations of a delta wing, *Journal of Aircraft*, 40(6), pp. 1206-1208, 2003.

[8] Peng, C. and Han, J.: Numerical investigation of the effects of structural geometric and material nonlinearities on limit-cycle oscillation of a cropped delta wing, *Journal of Fluids and Structures*, 27 (4), pp.611-622, 2011.

[9] Bungartz, et al.: preCICE – A fully parallel library for multi-physics surface coupling, *Computers & Fluids*, 141, pp.250-258, 2016.

[10] Takahashi, Y.: Large-Deformation Limit-Cycle Oscillation of a Delta Wing using Fluid-Structure Interaction Analysis at Transonic Speed, *Available at SSRN 4135441*.

[11] Economon, T.D., Palacios F., Copeland, S.R., Lukaczyk, T.W. and Alonso, J.J.: SU2: An open-source suite for multiphysics simulation and design, *AIAA Journal*, 54(3), pp.828-846, 2016.

[12] Dhondt, G. and Wittig, K.: Calculix – a free software three-dimensional structural finite element program, www.calculix.de.

[13] Jameson, A.: Origins and further development of the Jameson-Schmidt-Turkel scheme, *AIAA Journal*, 55(5), pp.1487-1510, 2017.

[14] Miranda, I. and Ferencz, R.M. and Hughes, T.J.R.: An improved implicit-explicit time integration method for structural dynamics, *Ear. Engrg. Stru. Dyn.*, 18(5), pp.643-653, 1989.